Measurements of the Birefringence and Verdet Constant in an Air-Core Fiber

He Wen, Matthew A. Terrel, Hyang Kyun Kim, Michel J. F. Digonnet, *Member, IEEE*, and Shanhui Fan, *Senior Member, IEEE*

***Abstract*—In order to determine the Verdet constant of an air-core photonic bandgap fiber (PBF), the birefringence of the fiber needs to be accurately known. We used two methods to measure the linear and circular birefringence of a commercial PBF around 1.5 μm. The linear birefringence beat length is found to vary significantly with wavelength, ranging from 6.8 $\pm$ 0.2 cm at 1526.8 nm to 9.5 $\pm$ 0.4 cm at 1596.8 nm. The circular birefringence is observed to be weaker by a factor of at least ten. The Verdet constant of this fiber, measured using a Faraday-effect measurement, is 6.1 $\pm$ 0.3 mrad/T/m. This value is in broad agreement with the prediction of a numerical model, and it confirms that the Verdet constant of this fiber is dominated by the residual spatial overlap of the mode with silica. It is also found to be 90 times weaker than the Verdet constant of a solid-core fiber (SMF-28) measured by the same process (0.55 $\pm$ 0.01 rad/T/m, in agreement with published values). This significantly reduced susceptibility to magnetic fields points to yet another benefit of air-core fibers in the fiber optic gyroscope.**

***Index Terms*—Birefringence, Faraday effect, optical fiber, photonic bandgap fibers.**

I. Introduction

In ALL applications of the fiber optic gyroscope (FOG), the sensing fiber is exposed to the Earth's magnetic field. Through the Faraday effect present in the fiber silica, this magnetic field induces a differential phase shift between the waves counterpropagating in the sensing coil [1]. Because the field varies over time and space, and because the sensing coil often moves in space, this effect results in a drift in the FOG output signal that is indistinguishable from a rotation. Although the Faraday effect in silica is weak, it is strong enough to be troublesome in high-sensitivity FOGs, in particular for aircraft inertial navigation. This problem is typically handled by placing the sensing coil in a μ-metal enclosure, which shields off the magnetic field, but this solution increases the size, weight, and cost of the gyro.

We have pointed out that the Faraday effect, as well as other undesirable effects such as thermal drift, can be significantly reduced by replacing the solid-core, index-guided fiber used in a conventional FOG by an air-core photonic-bandgap fiber (PBF) [2]. In such a fiber, most of the energy of the fundamental mode is confined in air, which has a much lower Verdet constant than silica. Consequently, the effective Verdet constant seen by this mode is expected to be much lower than in a conventional fiber, in which all of the mode energy travels through silica. Hence, the use of an air-core fiber in the sensing coil would significantly reduce the magnetic-field-related long-term drift in a fiber gyro. In this paper, we confirm this prediction by reporting the first measurement of the Verdet constant of the fundamental mode of an air-core fiber (Crystal Fibre's HC-1550-02 fiber).

Measurement of the Verdet constant in a fiber that exhibits birefringence requires accurate knowledge of its linear and circular birefringence. To date, the very few studies of an air-core fiber birefringence, theoretical and experimental, all show that the birefringence is significant and varies greatly with wavelength and from fiber to fiber. Wegmuller *et al.* reported a measured beat length of 1.1 cm for a 1.55-μm hollow-core fiber with a nominally circular core [3]. Polarization properties such as birefringence, polarization-dependent loss, and polarization-mode dispersion were all found to be strongly influenced by the presence of surface modes in the bandgap [3]. This behavior was confirmed by independent numerical simulations of birefringence by Poletti *et al.* [4]. In an 850-nm fiber with a slightly elliptical core (0.85:1), the beat length was found to range from 0.4 to 1.3 cm across the bandgap [5]. In the light of this wide range of birefringence, as part of our Verdet constant measurement, it was therefore essential that we measure the birefringence of our fiber.

This paper is arranged in four parts. In Section II, we report measurements of the fiber linear and circular birefringence. In Section III, we present a simple model that predicts the value of the Verdet constant of the HC-1550-02 fiber based on a numerical model of its fundamental mode profile. Section IV describes the experimental setup used to measure the Verdet constant. Section V presents the theory used to extract the Verdet constant from this measurement. Experimental results are reported in Section VI, and conclusions in Section VII.

II. Linear and Circular Birefringence Measurement

The test fiber HC-1550-02 has an air core with a diameter of 10.9 μm, surrounded by a photonic crystal cladding made of a triangular lattice of airholes with a period of 3.8 μm. Its photonic bandgap extends from $\sim$1520 to $\sim$1680 nm. This fiber is not truly single-mode at the testing wavelength range, but the few higher order modes are so lossy that the output of even the short lengths of fiber used in this work contains only the fundamental mode.

Manuscript received July 15, 2008; revised September 22, 2008. First published April 21, 2009; current version published July 20, 2009. This work was supported by Litton Systems, Inc., wholly owned by subsidiary of Northrop Grumman.

The authors are with the Edward L. Ginzton Laboratory, Stanford University, Stanford, CA 94305 USA (e-mail: vickywen@stanford.edu; terrel@stanford.edu; hkkim@stanford.edu; silurian@stanford.edu; shanhui@stanford.edu).

Digital Object Identifier 10.1109/JLT.2008.2009546

We used two methods to measure birefringence. The first one consists of launching single-frequency light of known polarization into a sub-beat-length section of fiber and measuring the output state of polarization (SOP) for linear input polarizations of different orientation. From this data, the Jones matrix of the fiber can be recovered, giving the linear and circular birefringence of the fiber at the measurement wavelength. The second method uses a white-light source measurement: linearly polarized white light is launched into the fiber, and the output spectrum is filtered through a polarizer. This spectrum exhibits fringes, which give information about the birefringence of the fiber. The purpose of this second measurement was simply to confirm the results of the Jones matrix measurements, which tends to be a little noisy.

The Jones matrix of a section of birefringent fiber, written in an arbitrary laboratory reference frame, is [6]

$$M = \begin{pmatrix} A & B \\ -B* & A* \end{pmatrix}$$
$$A = \cos(\Delta) + i\frac{\beta}{2}\frac{\sin(\Delta)}{\Delta}$$
$$B = -\left(\frac{\alpha}{2} + \frac{i\gamma}{2}\right)\frac{\sin(\Delta)}{\Delta}$$
$$\Delta = \frac{1}{2}\sqrt{\alpha^2 + \beta^2 + \gamma^2} \quad (1)$$

where α is the circular phase delay in the fiber section, β is the linear phase delay oriented along the x-axis, and γ is the linear phase delay oriented at 45° to the x-axis. The matrix above contains no explicit dependence on the length L of the fiber, but Δ is connected to the length L and beat length L_b of the fiber via $2\Delta = 2\pi L/L_b$. In order to measure the Jones matrix, the output polarizations (angle and ellipticity) must be measured for at least two known input polarizations. If 2Δ is known within 2π, then the values of the phase delays α, β, and γ can be determined uniquely from the Jones matrix. If 2Δ is uncertain modulus 2π, multiple values for α, β, and γ are possible, and additional information is required to determine these parameters uniquely. Previous measurements made by twisting the HC-1550-02 fiber and measuring the Jones matrix of very short (<1 cm) fiber sections indicated that L_b is greater than 6.5 cm over the wavelength range under consideration [7]. Consequently, in the Jones matrix measurements, we used a 2.8 cm length of fiber (cut from the same coil used in the white-light experiment) to ensure that $-\pi/2 < \Delta < +\pi/2$.

The Jones matrix measurements were carried out with an Agilent 8509c polarization analyzer. The 2.8-cm fiber sample was fixed in a mount, and light from a tunable laser was coupled into its core with a lens. For a given wavelength, 12 different linear input polarizations, spaced 15° apart, were launched into the PBF, and the resulting output polarizations were measured. The Jones matrix was then found in a fitting procedure by varying α, β, and γ and minimizing the total difference between measured and fit output polarizations. This procedure was repeated for 12 wavelengths between 1526.8 and 1596.8 nm. It was observed that small changes in the system alignment changed the measured birefringence. Therefore, several measurements (five to eight) of the Jones matrix were performed at each wavelength to evaluate the error of each data point.

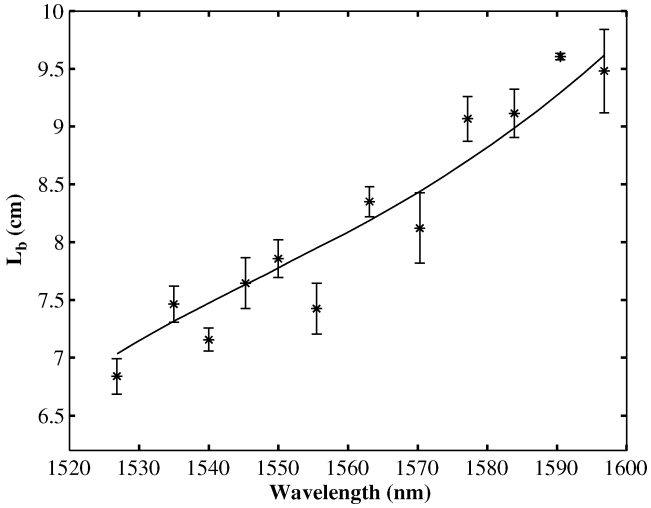

Fig. 1. Measured linear-birefringence beat length as a function of wavelength. Points are measurements from the Jones matrix method. Solid curve is from the white-light method.

Fig. 1 shows the measured beat length of the linear birefringence of this fiber. It shows that the linear birefringence is significant, with a beat length of about 8 cm at 1570 nm. This is a significantly longer beat length than previously reported for different air-core fiber [3]. The birefringence also varies significantly with wavelength. Since an ideal symmetric fiber should in theory exhibit no birefringence [8], this relatively strong birefringence indicates that the sixfold rotational symmetry is not preserved in the fiber structure. Because the majority of the optical power travels in the air core, it is likely that this birefringence is not due to strain within the fiber but to geometrical deformation of the fiber core region.

The white-light method uses the wavelength dependence of the phase difference $\Delta\phi(\lambda)$ between the two polarization eigenstates of the fiber in order to obtain information about the birefringence Δn and its variation with wavelength. A diagram of the experiment is shown in Fig. 2. Linearly polarized broadband light (amplified spontaneous emission from an Erbium (Er)-doped fiber) was launched into a 5.5-m length of the same air-core PBF wrapped in a coil of 10-cm radius (bending has little effect on the birefringence of this fiber, as no additional birefringence was observed using a coil of 2-cm radius). The output of the fiber was passed through a second polarizer, then coupled into a section of standard single-mode fiber (Corning's SMF-28) using bulk optics, and finally sent into an optical spectrum analyzer. The SMF-28 fiber section serves as a mode filter, eliminating the possible contribution of other modes in the PBF besides the fundamental mode. The polarizer angles were adjusted to give maximum contrast in the measured output spectrum. To compensate for the strong wavelength dependence of the input power from the broadband source, this measured spectrum (P_2) was normalized to the power spectrum (P_1) measured with the same setup except without the output polarizer.

A representative normalized output spectrum is shown in Fig. 3. It exhibits the expected periodic transmission as a function of wavelength that result from the variation of $\Delta\phi(\lambda)$ with λ.

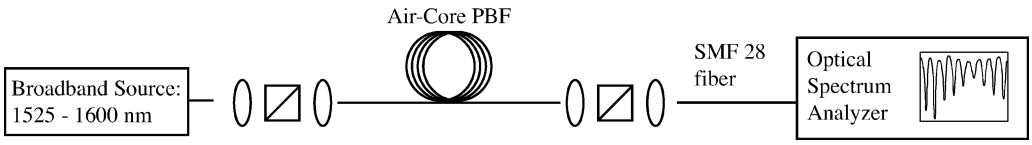

Fig. 2. Experimental setup for the white-light method.

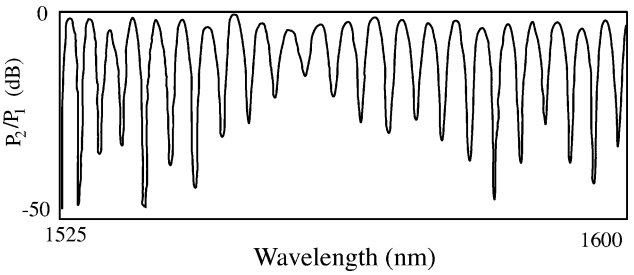

Fig. 3. Normalized output spectrum measured with the while-light source.

The phase difference $\Delta\phi$ between two adjacent peaks of the normalized white-light spectrum located at wavelengths λ_j and λ_{j+1} is $\pm 2\pi$, i.e.,

$$\Delta\phi(\lambda_{j+1}) - \Delta\phi(\lambda_j) = 2\pi\left(\frac{\Delta n(\lambda_{j+1})}{\lambda_{j+1}} - \frac{\Delta n(\lambda_j)}{\lambda_j}\right) = \pm 2\pi. \tag{2}$$

From (2), we see that the white-light transmission spectrum is not sufficient to uniquely determine $\Delta n(\lambda)$. In order to obtain $\Delta n(\lambda)$ using (2), we must also know the sign of the right-hand side, as well as $\Delta n(\lambda)$ at one of the peak wavelengths. These two pieces of information are conveniently provided by our Jones matrix measurements. Specifically, first, since these measurements show that the beat length increases with wavelength, the right-hand side of (2) should be negative. Second, to determine the value of L_b at a particular wavelength, we used the value of $L_b = 7.7$ cm measured at $\lambda = 1550$ nm (see Fig. 1), which minimizes the mismatch between the white-light and Jones matrix data. Analysis of the white-light measurement data with these two pieces of information yielded the solid curve in Fig. 1. The white-light method yields the total beat length, which depends on both the linear and circular phase delays. In this fiber, the circular phase delay is so small that the total and linear beat lengths differ by less than 1%, so the blue curve shows essentially the linear-birefringence beat length. There is clearly excellent agreement between the two methods. Specifically, the slopes of the two measurements agree well. The agreement in the absolute location of the solid curve is strictly the result of having fitted the white-light data at a particular wavelength (1550 nm) to the Jones matrix data.

The rapid variation between the data points measured with the Jones matrix method (see Fig. 1) is most likely due to experimental error caused by slight misalignments of the fiber, polarization-dependent coupling, and/or coupling into bulk and surface modes. If the true birefringence of the fiber actually exhibited such rapid variations, then the white-light spectrum (Fig. 3) would exhibit rapid oscillation in wavelength regions where the birefringence changed quickly (e.g., between 1570 and 1577 nm), which is certainly not the case.

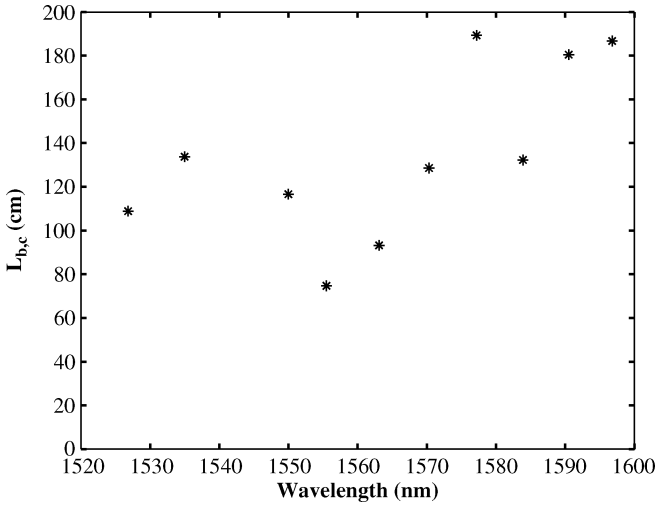

Fig. 4. Beat length of the circular birefringence.

The Jones matrix method allows us to quantify the relative contributions of circular and linear birefringence in the fiber. Fig. 4 shows the beat length of the circular birefringence, which is calculated from the circular phase delay α using the formula $L_{b,c} = 2\pi L/\alpha$. The circular phase delay is small, and the errors in its measurement are large, which translates into large uncertainty in $L_{b,c}$. The important result is that while the circular birefringence is not negligible, the overall birefringence of the fiber is dominated by the linear component. The linear birefringence is observed to be at least ten times stronger than the circular birefringence in this fiber at all the wavelengths under consideration.

III. Test Fiber and Expected Verdet Constant

The main objective of this work was to measure the Verdet constant of the HC-1550-02 air-core fiber. For calibration purposes, we also conducted the same Verdet constant measurement on a short length of standard single-mode fiber (Corning's SMF-28 fiber), for which the Verdet constant is known. Reported measured values of the Verdet constant of single-mode silica fiber at 1.55 μm range approximately from 0.52 to 0.60 rad/T/m [9]–[11], which is comparable to the reported values of the Verdet constant of silica.

Numerical simulations show that in the HC-1550-02 fiber, less than $\sim$1% of the fundamental mode energy at 1.55 μm is contained in silica. The rest of it propagates in air, The Verdet constant of air at 1.55 μm is of the order of $1.9 \times 10^{-3}\,\mathrm{rad/T/m}$ [12], which is nearly 300 times weaker than the Verdet constant of silica. Consequently, the Verdet constant of this fiber is expected to be at most 1% of the Verdet constant of a single-mode silica fiber.

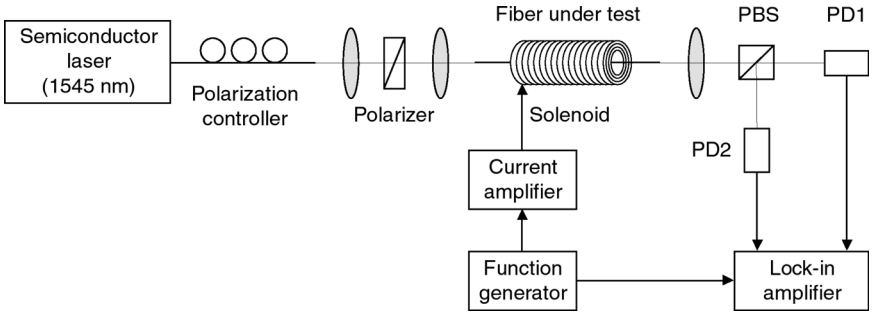

Fig. 5. Setup used to measure the Verdet constant of the air-core fiber. PD1 and PD2: photodetectors.

IV. Faraday Effect Measurement Setup

It is well known that through the Faraday effect, the application of a magnetic field to a material, in a direction parallel to the direction of propagation of light, induces a rotation of the polarization vector of the light proportional to the material's Verdet constant. The measurement of the Verdet constant of an optical fiber is therefore inherently simple: it involves measuring the change in the polarization of an optical signal as it travels through a short length of fiber exposed to a known magnetic field.

The measurement setup used to carry out this measurement, which is based on the configuration of [9], is depicted in Fig. 5. The polarized beam from a 1545-nm semiconductor laser was sent through a bulk-optic polarizer, then coupled into the test fiber. A fiber polarization controller placed at the output of the laser was used to adjust the SOP of the light entering the polarizer, and hence maximize the power transmitted by the polarizer. The fiber was placed along the axis of a solenoid, which generated the desired magnetic field. The solenoid was 10 cm long and consisted of ~611 m of 18-gauge wire. The signal exiting the fiber was split into two orthogonal, linearly polarized signals by a polarizing beam splitter (PBS) that could be rotated at an arbitrary angle about the fiber axis, and each signal was sent to a separate photodetector to measure its power. The quantity of interest in this measurement is $T = (P_2 - P_1)/(P_2 + P_1)$, where P_1 and P_2 are the powers in each signal [9]. The benefit of this two-signal measurement is that it eliminates certain sources of noise common to the two signals that are subtracted. Such common noise in particular includes power fluctuations of the laser and random temporal variations in the birefringence of the test fiber. In addition, the source that generated the switched solenoid current emitted electromagnetic noise, which was picked up by the photodetectors. This source of noise was also eliminated by this dual-detector scheme.

In the absence of magnetic field, the input polarizer was adjusted until the input polarization was aligned with one of the eigenstates of the fiber, i.e., until the output polarization was linear in the case of the SMF-28 fiber, and as close to linear as possible in the case of the PBF (which exhibits a small amount of circular birefringence). The PBS angle was then adjusted at 45° to this polarization, so that the powers measured by the two detectors P_1 and P_2 are equal. In the case of the SMF-28 fiber, since the output polarization is linear, at the end of this adjustment the parameter T was equal to 0. For the air-core fiber, the output signal was almost linearly polarized, and T was close to but not quite equal to 0, but by an amount so small that it had no bearing on the value of the Verdet constant ultimately inferred.

When a magnetic field is applied, the SOP of the output signal rotates, which modifies P_1 and P_2. The measurement therefore consists in turning on the field and, without changing the position of the PBS, measuring P_1 and P_2. To enhance the measurement signal-to-noise ratio (SNR), the solenoid current was modulated at $f = 10\,\mathrm{Hz}$, and the signals from the two photodetectors were analyzed with a dual-input lock-in amplifier (see Fig. 5). The latter provided the difference between the two signals $P_1 - P_2$, which was then normalized by the total detected power $P_1 + P_2$ to obtain T.

V. Theory for Calculating Verdet Constant

If a fiber is free of linear birefringence, the effect of a magnetic field is to rotate the state of polarization of light traveling through this fiber by an angle θ_m given by

$$Q_m = VBL \tag{3}$$

where L is the length of fiber exposed to the magnetic field, B is the component of the magnetic field along the fiber direction (z), assumed of constant amplitude, and V is the fiber's Verdet constant. However, when the fiber exhibits linear birefringence, it is well known that the polarization rotation angle is always smaller than this value and depends strongly on the birefringence [9]. The physical reason is that as a result of the combination of linear and circular birefringence, the signal SOP no longer remains linear along the entire fiber. Along at least portions of the fiber, the SOP has a circular component, and since a circular birefringence does not alter a circular polarization (it only changes its phase), the polarization rotation imparted to the signal is reduced. When the fiber birefringence and length are such that the signal spends equal amounts of time in the x and y polarizations in the magnetic field, since the rotation imparted on these two polarizations by a circular birefringence are equal and have opposite signs, there is no net rotation of the signal polarization. Consequently, for certain values of the linear retardation, the magnetic field has no effect on the output SOP. This shows that for a polarization rotation measurement to yield a reliable Verdet constant value, it is critical to accurately relate the measurand T to the quantity of interest θ_m.

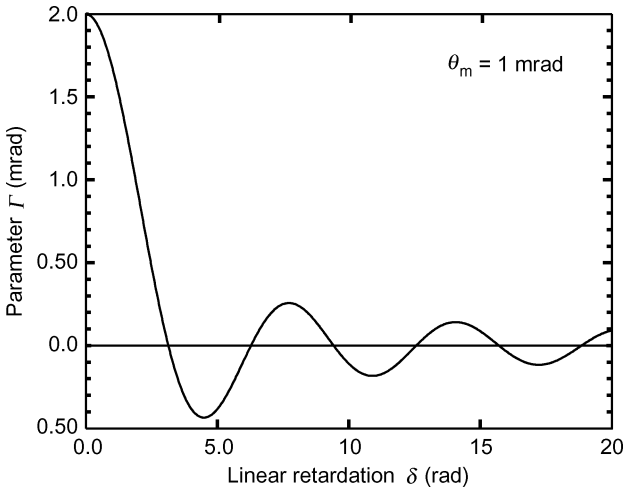

Fig. 6. Calculated dependence of the rotation angle θ on the fiber linear retardation δ.

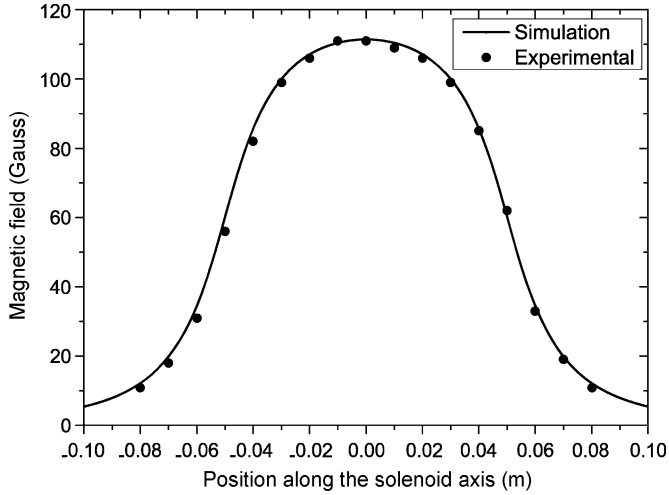

Fig. 7. Calculated and measured longitudinal dependence of the axial magnetic field along the solenoid axis.

When the magnetic field has a constant amplitude along the fiber, this relationship takes the simple form [13]:

$$T = 2\theta_m \frac{\sin\sqrt{\delta^2 + 4\theta_m^2}}{\sqrt{\delta^2 + 4\theta_m^2}} \tag{4}$$

where $\delta = 2\pi\Delta n L/\lambda$ is the phase retardation due to birefringence, Δn is the index birefringence of the fiber, and λ is the signal wavelength. For small angles θ_m, $T = 2\theta_m \sin\delta/\delta$, i.e., it is proportional to twice the Faraday rotation angle $2\theta_m$, and it varies with birefringence as $\sin\delta/\delta$. This dependence is plotted as the solid curve in Fig. 6 for a value of $\theta_m = 1$ mrad. As predicted above on physical grounds, for certain values of the retardation (or fiber length), the rotation vanishes. When the magnetically induced rotation angle is small ($\theta_m \ll \pi$), (4) states that these cancellations occur when δ is a multiple of π, i.e., when the fiber length is a multiple of half a beat length $L_b = \lambda/\Delta n$. This result implies that in order to be able to recover the Verdet constant from a polarization rotation measurement, the birefringence must be known fairly accurately.

The above dependence assumes that the field is constant along the fiber. In our experiment, however, this was not the case, for two reasons. First, coupling requirements imposed that the fiber extends a few centimeter out of the solenoid, on both sides of it. Second, the magnetic field generated by the solenoid was not constant along the solenoid axis z. This can be seen in Fig. 7, which plots the on axis magnetic field measured with a Gauss meter at a solenoid current of 0.29 A. The figure also shows the magnetic field calculated using basic electromagnetic theory, which required only the values of the solenoid's inner radius ($R_1 = 1$ cm), outer radius ($R_2 = 3.75$ cm), and length ($L_s = 10$ cm), and the estimated total number of turns in the winding ($N \approx 3740$). Theory and experiment agree and provide the absolute value of the field at any point along the test fiber required to recover the Verdet constant, as discussed below.

Since the field varies along the fiber length, (4) could not be used to relate T and θ_m. Instead, we calculated the exact polarization rotation in the presence of fiber birefringence for the actual magnetic field applied to the fiber (Fig. 7) by using the Jones matrix formalism. We divided the fiber in m imaginary segments of equal length $\Delta L = L/m$, short enough ($\sim$2 mm) that the field along a given segment i was equal to some essentially constant value B_i. We also assumed that both the linear and circular birefringence of the fiber were independent of position along the fiber, so that all segments had the same linear birefringence phase retardation and the same circular phase retardation. The Jones matrix of each segment, defined in the basis of the fiber's birefringence axes, is given by [6]

$$M_i = \begin{pmatrix} \cos\left(\frac{\Phi_i}{2}\right) - i\frac{\rho}{\Phi_i}\sin\left(\frac{\Phi_i}{2}\right) & -\frac{2F+\alpha}{\Phi_i}\sin\left(\frac{\Phi_i}{2}\right) \\ \frac{2F+\alpha}{\Phi_i}\sin\left(\frac{\Phi_i}{2}\right) & \cos\left(\frac{\Phi_i}{2}\right) + i\frac{\rho}{\Phi_i}\sin\left(\frac{\Phi_i}{2}\right) \end{pmatrix} \tag{5}$$

where i is the number of the segment ($i = 1$ to m), counted from the fiber input end, and

$$\begin{aligned} \Phi_i^2 &= \rho^2 + \alpha^2 + 4F_i^2 \\ F_i &= VB_i\Delta L \\ \alpha &= 2\pi\Delta L/L_{b,c} \\ \rho &= 2\pi\Delta L/L_b. \end{aligned} \tag{6}$$

The Jones matrix for the entire fiber is then the product of the m Jones matrices in reverse order:

$$M = \prod_{i=m}^{1} M_i. \tag{7}$$

Given this matrix and a known input signal (in this case, polarized along one of the birefringence axes), it is then easy to compute numerically the SOP of the fiber output signal, and from it the parameter T.

Simulations using (5) indicate that although the circular birefringence of the test fiber is small compared to the linear birefringence, when it is taken into consideration, the predicted value of T is reduced by 11%, which is not completely negligible. Consequently, to infer the Verdet constant from the measured value of T, we took the circular birefringence into account.

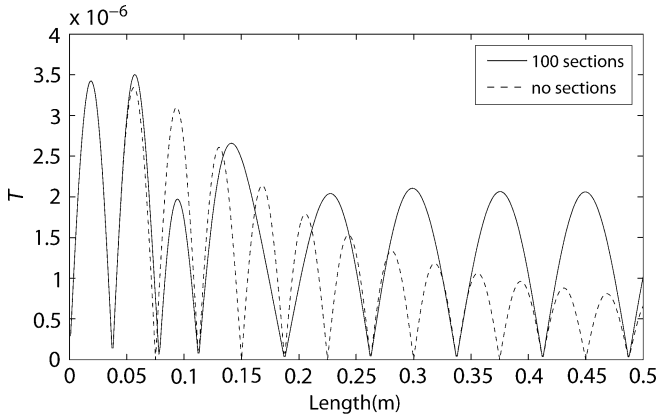

Fig. 8. Predicted detected signal T for both uniform field and nonuniform approaches.

The circular birefringence of the test PBF is likely due to random variations in the orientation of the principal axes of the fiber along its length. Hence, one does not expect the circular birefringence to be very uniform along z. Measurements of the circular birefringence on at least half a dozen different fiber samples indicate that the circular-birefringence beat length of this fiber is at least ten times greater than the linear-birefringence beat length. Hence, our assumption of a uniform circular-birefringence beat length of 75 cm represents a worst-case, and the small correction on T that it predicts (-11%) represents an upper bound value.

Fig. 8 plots the transmission T predicted for either a uniform field [(4)] or a nonuniform magnetic field integrated over 100 segments [(5)–(7)]. In both cases, the area under the magnetic field curve was taken to be the same. The two models agree up to a length of about one linear beat length, while for longer fibers the uniform-field predictions become increasingly inaccurate. The constant-field approximation clearly cannot be used when the length of the fiber exposed to the magnetic field is larger than one beat length. Since in our measurement the fiber had to be significantly longer than one beat length in order to obtain a strong enough output signal, we had to resort to the integrated field method to recover the Verdet constant from a measurement of T.

VI. Experimental Results

Fig. 9 shows the temporal evolution of the parameter Γ measured in a 15-cm length of SMF-28 fiber over a period of 20 min. (This parameter is the signal recorded directly from the lock-in amplifier; it must be normalized by the sum of the dc signals of two photodetectors to obtain parameter T.) During measurements, the modulated magnetic field was switched ON at a certain field strength, then switched OFF about 10 min later. The average value of Γ during the "ON" period inferred from Fig. 9 is 0.2 mV. The dc signal at each photodetector was 0.08 V, so after calibration of these two signals and normalization, the value of T was determined to be 1.26×10^{-3}.

Because the length of the solid-core fiber tested in the experiment is much shorter than its beat length, the uniform field approximation can be used in this case. Since the beat length of

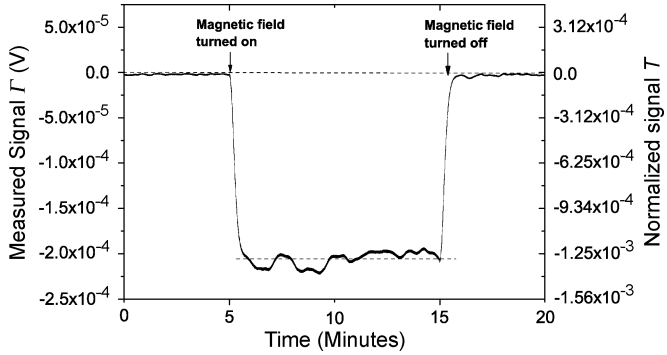

Fig. 9. Measured signal Γ and normalized signal T recorded for the SMF-28 fiber when the magnetic field was turned ON and OFF.

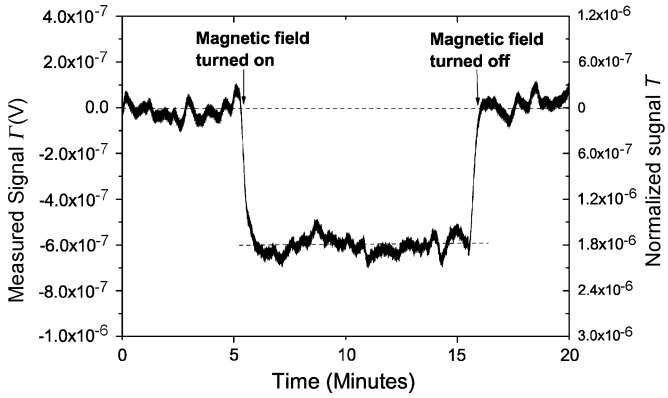

Fig. 10. Measured signal Γ and normalized signal T recorded for the air-core fiber when the magnetic field was turned ON and OFF.

SMF-28 fiber at 1.55 μm is $\sim$1.3 m, the linear retardation of the portion of fiber exposed to the field is $\delta = 2\pi L/L_b = 0.48$. Solving (4) for these values of T and δ yields $\theta_m = 0.66\,\mathrm{mrad}$. The solenoid current in this measurement was 0.29 A. The field integrated along the fiber $\int_L Bdl$ is 0.001 19 T.m. Inserting these values in (4), yields a Verdet constant for the SMF-28 fiber of 0.55 rad/T/m. This is in accord with the many values published for low-birefringence silica fibers at 1.55 μm, which range approximately from 0.52 to 0.60 rad/T/m [9]–[11]. This agreement lends credence to the calibration accuracy of our measurement technique.

The same measurement was repeated with a similar length of air-core fiber ($L = 13$ cm). The temporal evolution of Γ measured for this fiber at a solenoid current of 0.35 A is plotted in Fig. 10. Despite the large-applied field and long-exposed length of fiber, the signal was observed to be fairly noisy and weak, much more so than with the conventional fiber, suggesting that the Faraday effect in the air-core fiber is indeed quite weak, as anticipated.

The measured dependence of T on the magnitude of the applied field is plotted in Fig. 11. As expected, the dependence is linear, within experimental errors. After normalization, the slope of this curve gave a Verdet constant for the air-core fiber of 6.1 $\pm$ 0.3 mrad/T/m. This is 90 times weaker than the measured Verdet constant of the solid-core fiber, in agreement with the ratio of 100 expected from theory. Based on the values of the Verdet constants of air and silica, we conclude that this small

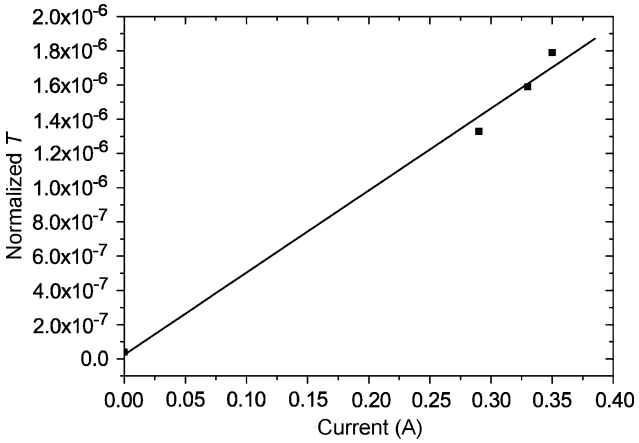

Fig. 11. Normalized signal recorded for the air-core fiber with varying current.

Verdet constant is dominated by the residual overlap of the fiber mode field with the silica membranes of the PBF.

VII. Conclusion

In order to measure the Verdet constant of a commercial air-core PBF, we conducted precise measurements of the birefringence of this fiber using both direct measurements of the Jones matrix of a short section of fiber and an independent white-light method. The linear birefringence was found to depend strongly on wavelength, with a beat length ranging from 6.8 to 9.5 cm over a wavelength range from 1526.8 to 1596.8 nm. The fiber's circular birefringence was found to be much weaker, with a beat length at least ten times longer. Using the measured birefringence, the Faraday effect experiment demonstrates that the Faraday rotation is much stronger in the solid-core fiber than that observed in the air-core fiber. The measured Verdet constant for the air-core fiber is $\sim 0.0061 \pm 0.003\ \mathrm{rad/T/m}$, which is much smaller than that of a solid-core fiber. The potential application of the air-core fiber in the FOG is obvious since the long-term drift due to Earth's magnetic field can be significant.

Acknowledgment

The authors would like to thank Y. He and L. Burns for their contributions to the initial stages of measurements, as well as Prof. J. M. Kahn for allowing to use his laboratory equipment for the Jones matrix measurements.

References

[1] K. Hotate and K. Tabe, "Drift of an optical fiber gyroscope caused by the Faraday effect: Influence of the Earth's magnetic field," *Appl. Opt.*, vol. 25, no. 7, pp. 1086–1092, Apr. 1986.

[2] H. K. Kim, M. J. F. Digonnet, and G. S. Kino, "Air-core photonic-bandgap fiber gyroscope," *J. Lighw. Technol.*, vol. 24, no. 8, pp. 3169–3174, Aug. 2006.

[3] M. Wegmuller, M. Legré, N. Gisin, T. Hansen, C. Jakobsen, and J. Broeng, "Experimental investigation of the polarization properties of a hollow core photonic bandgap fiber for 1550 nm," *Opt. Expr.*, vol. 13, pp. 1457–1467, Mar. 2005.

[4] F. Poletti, N. G. Broderick, D. Richardson, and T. Monro, "The effect of core asymmetries on the polarization properties of hollow core photonic bandgap fibers," *Opt. Expr.*, vol. 13, no. 22, pp. 9115–9124, Oct. 2005.

[5] G. Bouwmans, F. Luan, J. C. Knight, P. S. J. Russell, L. Farr, B. J. Mangan, and H. Sabert, "Properties of hollow-core photonic bandgap fiber at 850 nm wavelength," *Opt. Expr.*, vol. 11, no. 14, pp. 1613–1620, Jul. 2003.

[6] T. Chartier, A. Hideur, C. Özkul, F. Sanchez, and G. Stéphan, "Measurement of the elliptical birefringence of single-mode optical fibers," *Appl. Opt.*, vol. 40, pp. 5343–5353, Oct. 2001.

[7] M. Terrel, M. J. F. Digonnet, and S. Fan, "Polarization controller for hollow-core fiber," *Opt. Lett.*, vol. 32, pp. 1524–1526, May 2007.

[8] M. T. Steel, T. P. White, C. M. De Sterke, R. C. McPhedran, and L. C. Botten, "Symmetry and degeneracy in microstructured optical fibers," *Opt. Lett.*, vol. 26, pp. 488–490, Apr. 2001.

[9] A. M. Smith, "Polarization and magneto-optic properties of single-mode optical fiber," *Appl. Opt.*, vol. 17, no. 1, pp. 52–56, Jan. 1978.

[10] J. L. Cruz, M. V. Andres, and M. A. Hernandez, "Faraday effect in standard optical fibers: Dispersion of the effective Verdet constant," *Appl. Opt.*, vol. 35, no. 6, pp. 922–927, Feb. 1996.

[11] A. H. Rose, S. M. Etzel, and C. M. Wang, "Verdet constant dispersion in annealed optical fiber current sensors," *J. Lightw. Technol.*, vol. 15, no. 5, pp. 803–807, May 1997.

[12] D. Jacob, M. Vallet, F. Bretenaker, A. Le Floch, and R. La Naour, "The Malus Fabry–Perot interferometer," *Appl. Phys. Lett.*, vol. 66, no. 26, pp. 3546–3548, Jun. 1995.

[13] P. A. Williams, A. H. Rose, G. W. Day, T. E. Milner, and M. N. Deeter, "Temperature dependence of the Verdet constant in several diamagnetic glasses," *Appl. Opt.*, vol. 30, no. 10, pp. 1176–1178, Apr. 1991.

[14] G. W. Day, D. N. Payne, A. J. Barlow, and J. J. Ramskov-Hansen, "Faraday rotation in coiled, monomode optical fibers: Isolators, filters, and magnetic sensors," *Opt. Letters*, vol. 7, no. 5, pp. 238–240, May 1982.

He Wen received the B.A. Sc degree in electrical engineering from the University of British Columbia, Vancouver, Canada, in 2006. She is currently working toward the Ph.D. degree at the Department of Electrical Engineering, Stanford University, Stanford, CA.

Matthew A. Terrel received the B.S. degree in physics from the California Institute of Technology, Pasadena, in 2004, and the M.S. degree in applied physics from Stanford University, Stanford, CA, in 2006.

He is with the Edward L. Ginzton Laboratory, Stanford University. His current research interests include various aspects of optical fiber sensors.

Hyang Kyun Kim received the B.S. degree in physics from Yonsei University, Seoul, South Korea, in 1987, and the M.S. and Ph.D. degrees in physics from the Korea Advanced Institute of Science and Technology (KAIST), Taejon, South Korea, in 1990 and 1994, respectively.

From 1994 to 1999, she was with the Electronics and Telecommunication Research Institute (ETRI), Taejon, South Korea, as a Senior Research Engineer. From 1999 to 2000, he was a Member of Technical Staff, Bell Labs, Lucent Technologies, NJ. From 2001 to 2002, he was a Principal Staff Engineer, Novera Optics, CA. Since 2002, she has been with the Edward L. Ginzton Laboratory, Stanford University, Stanford, CA, as a Research Associate. Her current research interests include various aspects in fiber optic communication systems and optical fiber sensors. She is also involved in photonic-crystal fibers and designing, characterization, and applications for sensors/communication systems and fiber optic components.

Michel J. F. Digonnet (M'01) received the degree of engineering from the Ecole Supérieure de Physique et de Chimie de la Ville de Paris, Paris, France, and the Diplome d'Etudes Approfondies in coherent optics from the University of Paris, Orsay, France, in 1978, and the Ph.D. degree from the Applied Physics Department, Stanford University, Stanford, CA, in 1983. His doctoral research centered on wavelength-division multiplexing (WDM) fiber couplers and single-crystal fiber lasers and amplifiers.

From 1983 to 1986, he was with the Litton Guidance and Control, Chatsworth, CA, where he was engaged in research on miniature solid-state sources and integrated optics for fiber sensors. From 1986 to 1990, he was involved in the development of dye and 2-μm solid-state lasers, fiber sensors, and delivery systems for laser angioplasty at MCM Laboratories, Mountain View, CA. Since then, he has been a Senior Research Associate in Stanford University's Applied Physics Department. He is the author or coauthor of more than 220 articles published, issued 65 patents, edited several books, taught courses in fiber amplifiers, lasers, and sensors, and chaired numerous conferences on various aspects of photonics. His current research interests

include photonic bandgap fibers, fiber sensors and sensor arrays, high-power ceramic lasers, fiber lasers and amplifiers, and slow light in fibers.

Shanhui Fan (M'05–SM'06) received the Ph.D. degree in physics from the Massachusetts Institute of Technology (MIT), Cambridge, in 1997.

From 1988 to 1992, he was an undergraduate student in physics at the University of Science and Technology of China, Hefei, Anhui, China. From 1997 to 1999, he was a Postdoctoral Research Associate of Physics at MIT. During 1999 to 2001, he was with the Research Laboratory of Electronics, MIT, as a Research Scientist. Since 2001, he has been with Stanford University, Stanford, CA, as an Associate Professor of Electrical Engineering. He is the author or coauthor of more than 140 published in journal articles, has given more than 100 invited talks, and is the holder of 28 granted U.S. Patents. His current research interests include theory and simulations of photonic and solid-state materials and devices, photonic crystals, nanoscale photonic devices and plasmonics, quantum optics, computational electromagnetics, and parallel scientific computing.

Dr. Fan received the Adolph Lomb Medal from the Optical Society of America, the National Academy of Sciences Award for Initiative in Research, a David and Lucile Packard Fellowship, and a National Science Foundation Career Award. He is a fellow of Optical Society of America (OSA) and a member of American Physical Society (APS) and The International Society for Optical Engineers (SPIE).